Proceedings of DETC'99
1999 ASME Design Engineering Technical Conferences
September 12-15, 1999, Las Vegas, Nevada, USA

DETC99/VIB-8318

BIFURCATIONS IN THE DYNAMICS OF TWO COUPLED VAN DER POL OSCILLATORS WITH DELAY COUPLING

Stephen Wirkus
Center for Applied Mathematics
Cornell University
Ithaca, NY 14853
Email: saw8@cornell.edu

Richard Rand
Department of Theoretical and Applied Mechanics
Cornell University
Ithaca, NY 14853
Email: rhr2@cornell.edu

ABSTRACT

We investigate the dynamics of a system of two van der Pol oscillators with delayed velocity coupling. We use the method of averaging to reduce the problem to the study of a slow-flow in three dimensions. We study the steady state solutions of this slow flow, with special attention given to the bifurcations accompanying their change in number and stability. Our interest in this system is due to its relevance to coupled laser oscillators.

INTRODUCTION

This work is concerned with the mutual interaction of two limit cycle oscillators. It is motivated by applications to laser dynamics (York and Compton, 1992), (York 1993), (Lynch and York, 1995), (Lynch, 1995). When two lasers operate physically close to one another, the light output of each may affect the behavior of the other. Since the frequencies of some lasers are in the 10 GHz range, the time for light to travel from one laser to the other, a distance of the order of cm, represents a substantial portion of the period of the uncoupled laser oscillator. This immediately leads to the inclusion of delay effects in the coupling terms.

In this paper we investigate the dynamics of two weakly coupled van der Pol oscillators in which the coupling terms have time delay τ. We use the method of averaging to obtain an approximate simplified system of three slow flow equations and then investigate the stability and bifurcation of their equilibria (corresponding to periodic motions in the original system).

This work is an extension of a previous paper by the present authors (Wirkus and Rand, 1997) and is also related to previous studies of coupled van der Pol oscillators in which the coupling terms omitted delay effects (Rand and Holmes, 1980), (Storti and Rand, 1982), (Storti and Rand, 1986),(Chakraborty and Rand, 1988).

DERIVATION OF SLOW FLOW EQUATIONS

We investigate two van der Pol oscillators with delay coupling (York 1993),(Lynch and York, 1995):

$$\ddot{x}_1 + x_1 - \epsilon\ (1 - x_1^2)\ \dot{x}_1 = \epsilon\ \alpha \dot{x}_2\ (t - \tau), \qquad (1)$$

$$\ddot{x}_2 + x_2 - \epsilon\ (1 - x_2^2)\ \dot{x}_2 = \epsilon\ \alpha \dot{x}_1\ (t - \tau). \qquad (2)$$

where α is a coupling parameter, τ is the delay time, and where $\epsilon << 1$. When $\epsilon = 0$, the system reduces to $\ddot{x}_i + x_i = 0, i = 1, 2$, with solution:

$$x_i\ =\ R_i\ \cos(t + \theta_i), \qquad \dot{x}_i\ =\ -\ R_i\ \sin(t + \theta_i). \quad (3)$$

For $\epsilon > 0$, we look for a solution in the form (3) but treat R_i and θ_i as time dependent. Variation of parameters gives the following eqs. on R_i and θ_i:

$$\dot{R}_i = -\epsilon\ \sin(t + \theta_i)\ F_i, \quad R_i\ \dot{\theta}_i = -\epsilon\ \cos(t + \theta_i)\ F_i \quad (4)$$

where $F_i\ =\ (1 - x_i^2)\ \dot{x}_i + \alpha\ \dot{x}_j(t - \tau), i, j = 1, 2$. For small ϵ we use the method of averaging, replacing the right hand sides of (4) by their averages over one period of the $\epsilon = 0$

system:

$$\dot{R}_i \approx -\epsilon \ \frac{1}{2\pi} \int_0^{2\pi} \sin(t+\theta_i) \ F_i \ dt, \tag{5}$$

$$R_i \ \dot{\theta}_i \approx -\epsilon \ \frac{1}{2\pi} \int_0^{2\pi} \cos(t+\theta_i) \ F_i \ dt, \tag{6}$$

in which

$$F_i = [1 - R_i^2 \ \cos^2(t+\theta_i)] \ [-R_i \ \sin(t+\theta_i)] + \alpha \ [-\tilde{R}_j \ \sin(t-\tau+\tilde{\theta}_j)], \tag{7}$$

where $\tilde{R} = R(t-\tau)$ and $\tilde{\theta} = \theta(t-\tau)$. Evaluating the integrals $\oint \cos(t+\theta_i) \ F_i \ dt$ and $\oint \sin(t+\theta_i) \ F_i \ dt$ gives $(i \neq j)$

$$\dot{R}_i \ = \ \frac{\epsilon}{2} \ R_i \ (1 - \frac{R_i^2}{4}) + \frac{\epsilon \ \alpha}{2} \ \tilde{R}_j \ \cos(\theta_i - \tilde{\theta}_j + \tau), \tag{8}$$

$$R_i \ \dot{\theta}_i \ = \ -\frac{\epsilon \ \alpha}{2} \ \tilde{R}_j \ \sin(\theta_i - \tilde{\theta}_j + \tau). \tag{9}$$

Eqs. (8)-(9), show that $\dot{R}_i$,$\dot{\theta}_i$ are $O(\epsilon)$. We now Taylor expand $\tilde{R}_i$ and $\tilde{\theta}_i$:

$$\tilde{R}_i = R_i(t-\tau) = R_i(t) - \tau \dot{R}_i(t) + \tau^2 \ddot{R}_i(t) + \cdots, \tag{10}$$

$$\tilde{\theta}_i = \theta_i(t-\tau) = \theta_i(t) - \tau \dot{\theta}_i(t) + +\tau^2 \ddot{\theta}_i(t) + \cdots. \tag{11}$$

Eqs. (10),(11) indicate that we can replace $\tilde{R}_i$,$\tilde{\theta}_i$ by R_i,θ_i in eqs.(8),(9) since $\dot{R}_i(t)$,$\dot{\theta}_i(t)$ and $\ddot{R}_i(t)$,$\ddot{\theta}_i(t)$ in (10),(11) are $O(\epsilon)$ and $O(\epsilon^2)$ respectively, from eqs.(8),(9). This reduces an infinite dimensional problem in functional analysis to a finite dimensional problem by assuming the product $\epsilon\tau$ is small. (Note that we do not assume a small delay τ.) This key step enables us to handle the original system, a differential delay eq., as a system of differential eqs. (York and Compton, 1992),(York 1993),(Lynch and York, 1995),(Lynch, 1995). Note that if terms of $O(\epsilon^2)$ were retained in eqs. (10),(11), then the resulting differential equations would be of second order. Thus extending the expansion to higher order in ϵ has the unusual effect of profoundly changing the nature of the approximate system to be solved. Nevertheless the $O(\epsilon)$ truncation studied in this work is valid for small values of $\epsilon\tau$, as demonstrated by comparison of the subsequent slow flow analysis with numerical integration of the original differential delay eqs. (1),(2).

Setting $\phi \ = \ \theta_1 - \theta_2$, we then obtain

$$\dot{R}_1 = \frac{\epsilon}{2} \ [R_1 \ (1 - \frac{R_1^2}{4}) + \alpha \ R_2 \ \cos(\phi + \tau)], \tag{12}$$

$$\dot{R}_2 = \frac{\epsilon}{2} \ [R_2 \ (1 - \frac{R_2^2}{4}) + \alpha \ R_1 \ \cos(\phi - \tau)], \tag{13}$$

$$\dot{\phi} = \frac{\epsilon \ \alpha}{2} \ [-\frac{R_2}{R_1} \ \sin(\phi + \tau) - \frac{R_1}{R_2} \ \sin(\phi - \tau)]. \tag{14}$$

These are the slow-flow equations which we will examine in the remainder of the paper.

Note that R_1 and R_2 are nonnegative and the vector field associated with eqs.(12)-(14) is periodic in ϕ. Thus the phase space is $R^+ \times R^+ \times S^1$. The slow-flow is invariant under the three transformations:

$$(R_1, \ R_2, \ \phi) \mapsto (R_2, \ R_1, -\phi) \tag{15}$$

$$\phi \mapsto \phi + \pi, \qquad \alpha \mapsto -\alpha \tag{16}$$

$$\phi \mapsto \phi + \pi, \qquad \tau \mapsto \tau + \pi, \qquad \cos\tau \mapsto -\cos\tau. \tag{17}$$

Eqs.(16),(17) show that another invariance involving only parameters is:

$$\alpha \mapsto -\alpha, \qquad \tau \mapsto \tau + \pi, \qquad \cos\tau \mapsto -\cos\tau. \tag{18}$$

Eq.(18) shows that we may assume $\alpha > 0$ without loss of generality,since the phase flow for a negative value of α is identical to that of the corresponding positive value of α with the sign of $\cos\tau$ reversed.

STABILITY OF THE IN-PHASE MODE

Eqs.(12)-(14) possess the following equilibrium point which corresponds to the in-phase mode $x_1 \equiv x_2$ in (1),(2):

$$R_1 = R_2 = 2\sqrt{1 + \alpha \ \cos\tau}, \phi = 0; \ 1 + \alpha\cos\tau > 0. \tag{19}$$

Notice that eqs.(19) indicate that the amplitudes R_i approach zero as $1 + \alpha\cos\tau$ approaches zero, and that these

amplitudes remain zero for $1 + \alpha \cos\tau \leq 0$. This result is known as *amplitude death* (Reddy, Sen, and Johnston, 1998), (Strogatz, 1998). Thus the in-phase mode is predicted to come into existence as we cross the curve $\alpha = -1/\cos\tau$ in the $\cos\tau - \alpha$ parameter plane. This bifurcation is accompanied by a change in stability of the trivial solution $x_1 \equiv x_2 \equiv 0$. In order to show this we must return to the original differential delay eqs.(1),(2), since the slow flow (12)-(14) is singular for $R_1 = R_2 = 0$. Linearizing eqs.(1),(2) about the trivial solution, we may obtain the condition for a change in stability of $x_1 \equiv x_2 \equiv 0$ by assuming a solution of the form $e^{i\omega t}$. Equating real and imaginary parts of the corresponding characteristic equation, we obtain:

$$\cos\omega\tau = -\frac{1}{\alpha}, \qquad \sin\omega\tau = \frac{1-\omega^2}{\epsilon\alpha\omega}. \tag{20}$$

In the small ϵ limit, the second of eqs.(20) gives that $\omega = 1$, and then the first of eqs.(20) gives $\alpha = -1/\cos\tau$,in agreement with the birth of the in-phase mode, cf.eq.(19).

In order to determine the stability of the in-phase mode, we examine the eigenvalues λ of the Jacobian matrix of the right-hand side of eqs. (12)-(14) evaluated at the equilibrium (19). These satisfy the equation:

$$\begin{aligned}&\lambda^{\,3} + \lambda^2\,(2 + 4\,\alpha\,\cos\tau)\\ &+ \lambda\,(1 + 5\,\alpha\,\cos\tau + \alpha^2 + 4\,\alpha^2\,\cos^2\tau)\\ &+ (\alpha\cos\tau + 2\alpha^2\cos^2\tau + \alpha^2 + \alpha^3\cos\tau + \alpha^3\cos^3\tau) = 0.\end{aligned} \tag{21}$$

When $\lambda = 0$, eq.(21) gives conditions necessary for a saddle-node bifurcation. The resulting equation may be factored into three conditions:

$$\alpha = 0, \tag{22}$$

$$\alpha = \frac{-\cos\tau}{1 + \cos^2\tau}, \tag{23}$$

$$\alpha = \frac{-1}{\cos\tau}. \tag{24}$$

We can similarly set $\lambda = i\omega$ to obtain conditions necessary for a Hopf bifurcation. Omitting extraneous roots, we obtain:

$$\alpha = -\frac{1}{3\,\cos\tau}, \qquad \cos^2\tau < \frac{1}{2}. \tag{25}$$

Simulation reveals that the limit cycle created in the Hopf bifurcation (25) is unstable.

Eqs.(22)-(25) represent stability boundaries for the in-phase mode $x_1 \equiv x_2$ in the $\cos\tau - \alpha$ parameter plane. See Fig.1.

In order to check the stability results in Fig.1, we numerically simulated eqs.(12)-(14). The delay terms in eqs.(12)-(14) require that initial conditions be given for the time interval between $-\tau$ and 0. We handled this by allowing the two oscillators to run uncoupled from $t = -\tau$ to $t = 0$. This was accomplished by specifying $x(-\tau)$ and $\dot{x}(-\tau)$. This allowed us to obtain an *interval* of initial conditions $\mathbf{x}(t) = \mathbf{\Phi}(t), \ -\tau \leq t \leq 0$. Then at time $t = 0$, we started numerically integrating the *coupled* delay equations, which required that we take into account what happened τ time units ago. Here we use a fourth order Runge-Kutta scheme with fixed step size, appropriately modified to account for delay (Hairer et al., 1987). In order to avoid unnecessarily long runs, we began "close" to the equilibrium point whose stability we were investigating. For example, in the case of the in-phase mode, we took $x_1 \approx x_2$, $\dot{x}_1 \approx \dot{x}_2$. A point in $\cos\tau - \alpha$ parameter space is said to stable if the trajectory in four-dimensional phase space continues to spiral into the in-phase mode. In this way we were able to confirm that the stability of the in-phase and out-of-phase modes agreed with the predictions of the analytical method shown in Fig. 1.

STABILITY OF THE OUT-OF-PHASE MODE

In addition to the in-phase mode, eqs.(12)-(14) also possess an equilibrium which corresponds to the out-of-phase mode $x_1 \equiv -x_2$:

$$R_1 = R_2 = 2\sqrt{1 - \alpha\,\cos\tau}, \phi \;=\; \pi;\; 1 - \alpha\cos\tau > 0. \tag{26}$$

In order to determine the stability of this mode we could proceed in an analogous fashion to that used for the in-phase mode. However, a more direct approach is available to us due to the symmetry discussed in eqs.(16)-(18). The out-of-phase mode (26) maps to the in-phase mode (19) under the transformation (17), $\alpha \mapsto -\alpha$, $\tau \mapsto \tau + \pi$. But since the entire phase flow is invariant under this transformation, the stability of (26) is seen to be identical to that of (19) with the parameter change $\cos\tau \mapsto -\cos\tau$. That is, the out-of-phase mode has the same stability chart as the in-phase mode, reflected about the α-axis. See Fig.1.

OTHER PERIODIC MOTIONS

Having investigated the stability of the slow flow equilibria corresponding to in-phase and out-of-phase modes, we now look for any other slow flow equilibria, each of which corresponds to a periodic motion in the original eqs.(1),(2). Our task is to solve the three eqs.(12)-(14) for equilibrium values of R_1, R_2 and ϕ. We solve (13) for R_1, substitute the result into (14) and solve for R_2^2. Call the result "eq.A". Then we solve (13) for R_1 and substitute the result into (12), giving a polynomial on R_2^2. We substitute "eq.A" into this polynomial, giving an equation with no R_1 or R_2 in it. Algebraic and trigonometric simplification of the resulting equation gives:

$$\alpha^2 \sin^2\tau \cos^4\phi + (2\alpha^2 \sin^2\tau - 1)\cos^2\tau\cos^2\phi + \cos^4\tau(1+\alpha^2\sin^2\tau) = 0. \quad (27)$$

Eq.(27) is a quadratic on $\cos^2\phi$. We may obtain up to 4 real values for $\cos\phi$, corresponding to 8 values of ϕ. Of these 8, 4 must be rejected because they correspond to negative R_i values. The remaining 4 equilibria come in 2 pairs which map to each other under the transformation (15).

Bifurcations of these equilibria result from setting $\cos\phi = 1$ in eq.(27) since $\cos^2\phi \le 1$. This gives eq.(23) and its reflection in the symmetry (17). Bifurcations also occur in eq.(27) if the discriminant vanishes. This results in the condition:

$$\alpha^2 = \frac{1}{8(1-\cos^2\tau)}, \qquad \cos^2\tau < \frac{1}{3}. \quad (28)$$

Eq.(28) is displayed on Fig.2 along with the previously obtained bifurcation curves (23),(24),(25). Points P and Q in Fig.2 are defined as the points of intersection of curves (23),(25) and of curves (23),(28), respectively:

$$\text{P:}\ \ \cos\tau = -\frac{1}{\sqrt{2}},\ \alpha = \frac{\sqrt{2}}{3}, \qquad \text{Q:}\ \ \cos\tau = -\frac{1}{\sqrt{3}},\ \alpha = \frac{\sqrt{3}}{4}. \quad (29)$$

The total number of slow flow equilibria in eqs.(12)-(14) depends on the parameters α and τ, see Fig.2. The maximum number is 6, consisting of the in-phase mode, the out-of-phase mode, and the 4 additional equilibria associated with eq.(27). Note that none of these additional equilibria can occur if the coupling α is sufficiently large.

We checked these results by numerically simulating eqs.(12)-(14). In doing so we discovered that the equilibria discussed in this section undergo Hopf bifurcations in the regions marked '4' and '6' in Fig.2. In order to find the location of these Hopfs in the parameter plane of Fig.2, we linearized the slow flow eqs.(12)-(14) about the equilibria given by eq.(27) and then set $\lambda = i\omega$ in the associated eigenequation. The resulting equations were too complicated algebraically to allow us to obtain closed form conditions for the Hopfs (even using computer algebra). Nevertheless we were able to treat the resulting equations numerically, revealing that the Hopfs occur along a curve which is displayed in Fig.3. This curve is approximately given by the empirical equation:

$$\alpha = -0.045266\cos^4\tau + 0.286920\cos^2\tau + 0.3393455, \qquad 0.238095 \le \cos^2\tau \le 0.5. \quad (30)$$

As shown in Fig.3, the curve (30) reaches between point P and a point H on curve (28). The slow flow limit cycles which are born in these Hopfs correspond to quasiperiodic motions in the original eqs.(1),(2).

UNFOLDING POINT P

In order to better understand the bifurcations which occur in the slow flow eqs.(12)-(14), we magnify the region of parameter space around point P. This involves (i) expanding in power series the parameters α and τ about point P and the phase variables R_1, R_2 and ϕ about the in-phase equilibrium point, then (ii) transforming the phase variables to local eigencoordinates (which involve a double zero eigenvalue at point P), then (iii) obtaining a power series approximation for the center manifold at P, and then (iv) transforming the resulting two-dimensional flow to normal form. This is a very complicated calculation which involved a lot of computer algebra. We give only the final form of the flow on the center manifold:

$$\begin{aligned}
\dot{y} &= z \\
\dot{z} &= y^3(-\frac{1}{6} - \frac{175}{192}\sqrt{2}\mu - \frac{367}{288}\nu - \frac{1523}{256}\mu^2 + \frac{-317}{128}\nu^2 \\
&\quad - \frac{1945}{384}\sqrt{2}\mu\nu) + y^2 z(\frac{9}{2} + \frac{21}{4}\sqrt{2}\mu + \frac{19}{2}\nu - \frac{11763}{32}\mu^2 \\
&\quad + \frac{729}{16}\nu^2 - \frac{1029}{16}\sqrt{2}\mu\nu) \\
&\quad + y(-\frac{1}{2}\sqrt{2}\mu + \frac{1}{9}\nu - \frac{3}{2}\mu^2 - \frac{1}{6}\nu^2 + \frac{-1}{6}\sqrt{2}\mu\nu) \\
&\quad + z(\frac{3}{2}\sqrt{2}\mu + \nu - \frac{1}{2}\nu^2 + \frac{3}{2}\sqrt{2}\mu\nu). \quad (31)
\end{aligned}$$

where μ and ν are defined by the equations (cf.eq.(29)):

$$\tau = \arccos\left(-\frac{1}{\sqrt{2}}\right) + \nu, \qquad \alpha = \frac{\sqrt{2}}{3} + \mu. \tag{32}$$

Analysis of eq.(31) shows that there are 6 bifurcation curves which emanate from point P. See Fig.4 where these 6 curves are labeled A,B,C,D,E,F. Their description and approximate equations are found to be:

$$\text{A,C: pitchfork, eq.(23):} \quad \mu = \frac{\sqrt{2}}{9}\nu - \frac{13\sqrt{2}}{54}\nu^2 \tag{33}$$

$$\text{B: subcritical Hopf, eq.(25):} \quad \mu = -\frac{\sqrt{2}}{3}\nu + \frac{\sqrt{2}}{2}\nu^2 \tag{34}$$

$$\text{D: supercritical Hopf, eq.(30):} \quad \mu = \frac{\sqrt{2}}{6}\nu + \frac{47\sqrt{2}}{512}\nu^2 \tag{35}$$

$$\text{E: symmetry-breaking bifurcation:} \quad \mu = \frac{17\sqrt{2}}{93}\nu + \frac{38173\sqrt{2}}{178746}\nu^2 \tag{36}$$

$$\text{F: limit cycle fold :} \quad \mu = 0.26606\nu. \tag{37}$$

In curve E, the symmetry-breaking bifurcation, a pair of stable limit cycles is replaced by a single larger stable limit cycle. In curve F, the limit cycle fold, a pair of limit cycles, one stable and one unstable, coalesce. It will be noted that the algebraic form of curve F involves an approximate decimal, in contrast to the expressions for the other bifurcation curves. In fact a closed form expression for this constant is known in terms of elliptic integrals, but is omitted here for brevity. The details by which eqs.(33)-(37) are obtained, which involve Melnikov and elliptic integrals, are omitted here, but will be included in the doctoral thesis of the first author. Fig.5 shows a schematic of the bifurcation sequence obtained by moving through the parameter space near point P.

DISCUSSION

Perhaps the most significant result of this work is the conclusion that both the in-phase and out-of-phase modes are stable for values of $\cos\tau$ close to zero, i.e., for delays of about $\frac{1}{4}$ of the uncoupled period of the oscillators, see Fig.1. In applications where it is desirable to operate the system at the in-phase mode, the presence of a stable out-of-phase mode could be the source of unreliable behavior.

The elaborate bifurcation sequences which were found to be present in this system occur over a very small region of parameter space, and hence are not likely to be exhibited by an associated physical system. Nevertheless these bifurcations are important because they explain how dynamical transitions occur between the larger regions of parameter space.

The approximation used in this work is based on the assumption that $\epsilon\tau << 1$, and hence is not expected to give good results when this inequality is violated. In particular, the parameter τ always appears in the form $\cos\tau$ in the slow flow (12)-(14), leading to the prediction that the dynamical behavior exhibits a periodic dependence on τ. Recent research work which does not assume that $\epsilon\tau$ is small has shown that this prediction is only approximately true (Moon and Johnson, 1998), (Yeung and Strogatz, 1999).

ACKNOWLEDGMENT

The authors wish to thank Professor Rick Compton for proposing this problem, and Professor Steven Strogatz for helpful suggestions.

REFERENCES

Chakraborty,T. and Rand,R.H. The transition from phase locking to drift in a system of two weakly coupled van der Pol oscillators, Int. J. Nonlinear Mechanics 23:369-376, 1988.

Hairer,E., Norsett,S.P., and Wanner,G. *Solving Ordinary Differential Equations I: Nonstiff Problems*, Springer-Verlag, 1987.

Lynch,J.J. *Analysis and design of systems of coupled microwave oscillators,* Ph.D.thesis, Dept.Electrical and Computer Engineering, University of California at Santa Barbara, 1995.

Lynch,J.J. and York,R.A. Stability of mode locked states of coupled oscillator arrays, IEEE Trans. on Circuits and Systems 42:413-417, 1995.

Moon,F.C. and Johnson,M.A. Nonlinear dynamics and chaos in manufacturing processes, in *Dynamics and Chaos in Manufacturing Processes,* ed.F.C.Moon, Wiley, pp.3-32, 1998.

Rand,R.H. and Holmes,P.J. Bifurcation of periodic mo-

tions in two weakly coupled van der Pol oscillators, Int. J. Nonlinear Mechanics 15:387-399, 1980.

Reddy,D.V.R., Sen,A., and Johnston,G.L. Time delay induced death in coupled limit cycle oscillators, Physical Review Letters 80:5109-5112, 1998.

Storti,D.W. and Rand,R.H. Dynamics of two strongly coupled van der Pol oscillators, Int. J. Nonlinear Mechanics 17:143-152, 1982.

Storti,D.W. and Rand,R.H. Dynamics of two strongly coupled relaxation oscillators, SIAM J. Applied Math. 46:56-67, 1986.

Strogatz,S.H. Death by delay, Nature 394:317-318, 1998.

Wirkus,S. and Rand,R. Dynamics of two coupled van der Pol oscillators with delay coupling, Proceedings of DETC'97, 1997 ASME Design Engineering Technical Conferences, Sept.14-17,1997, Sacramento, CA, paper no.DETC97/VIB-4019.

Yeung,M.K.S. and Strogatz,S. Time delay in the Kuramoto model of coupled oscillators, Physical Review Letters 82:648-651, 1999.

York,R.A. Nonlinear analysis of phase relationships in quasi-optical oscillator arrays, IEEE Trans. on Microwave Theory and Tech. 41:1799-1809, 1993.

York,R.A. and Compton,R.C. Experimental observation and simulation of mode-locking phenomena in coupled-oscillator arrays, J.Appl.Phys. 71:2959-2965, 1992.

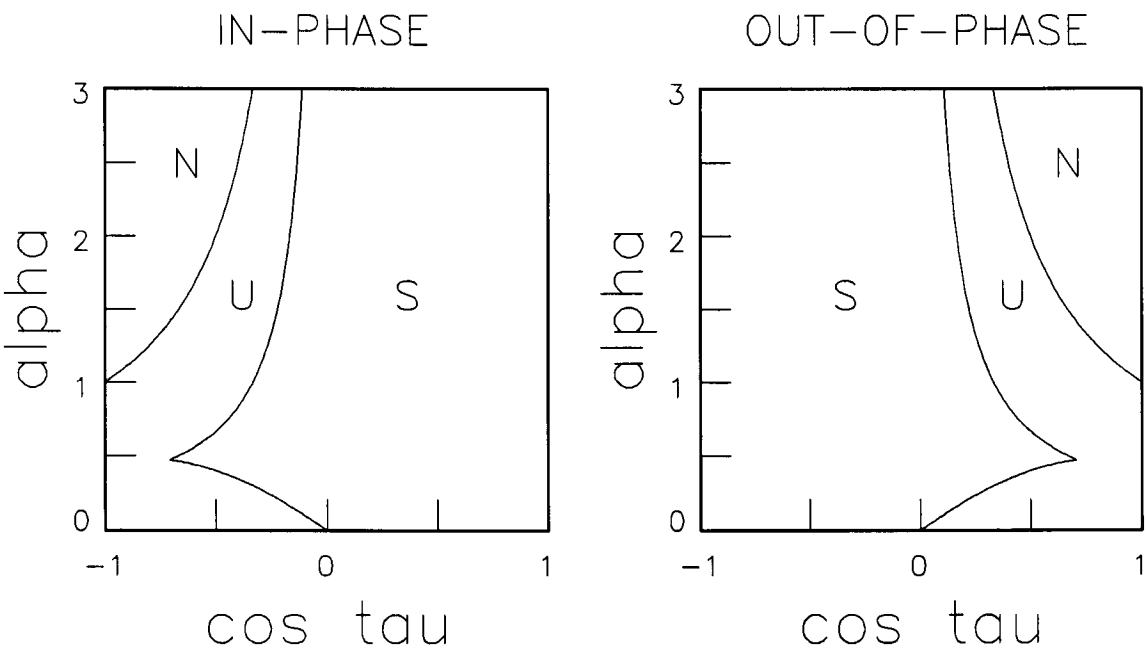

Figure 1. Stability of the in-phase and out-of-phase modes.
S=stable, U=unstable, N=does not exist.

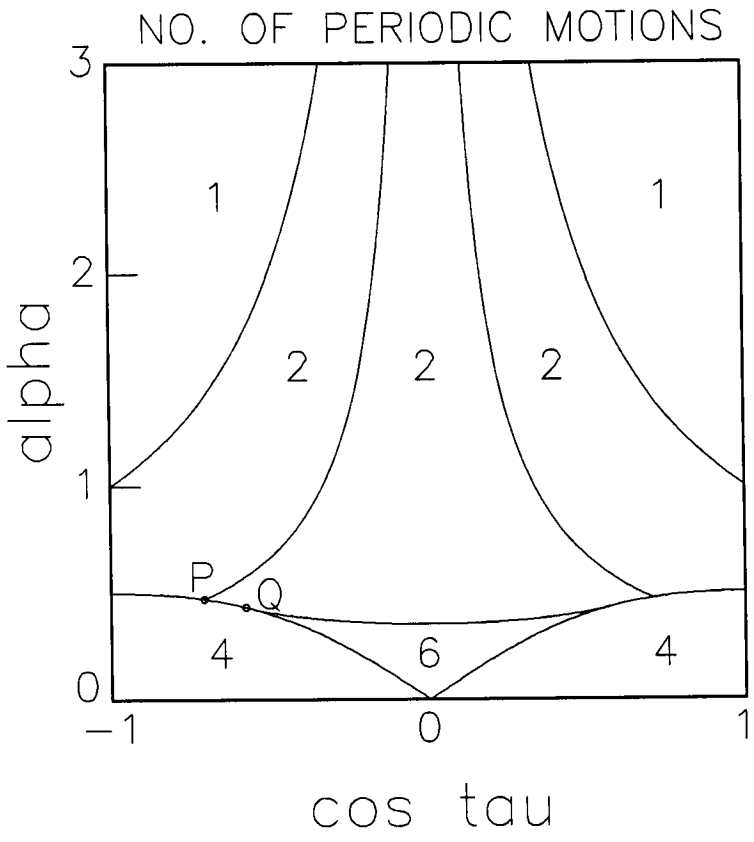

Figure 2. Number of periodic motions exhibited by the slow flow (12)-(14).
The displayed curves are the bifurcation eqs.(23),(24),(25),(28),
as well as their reflections in the $\alpha-$axis.

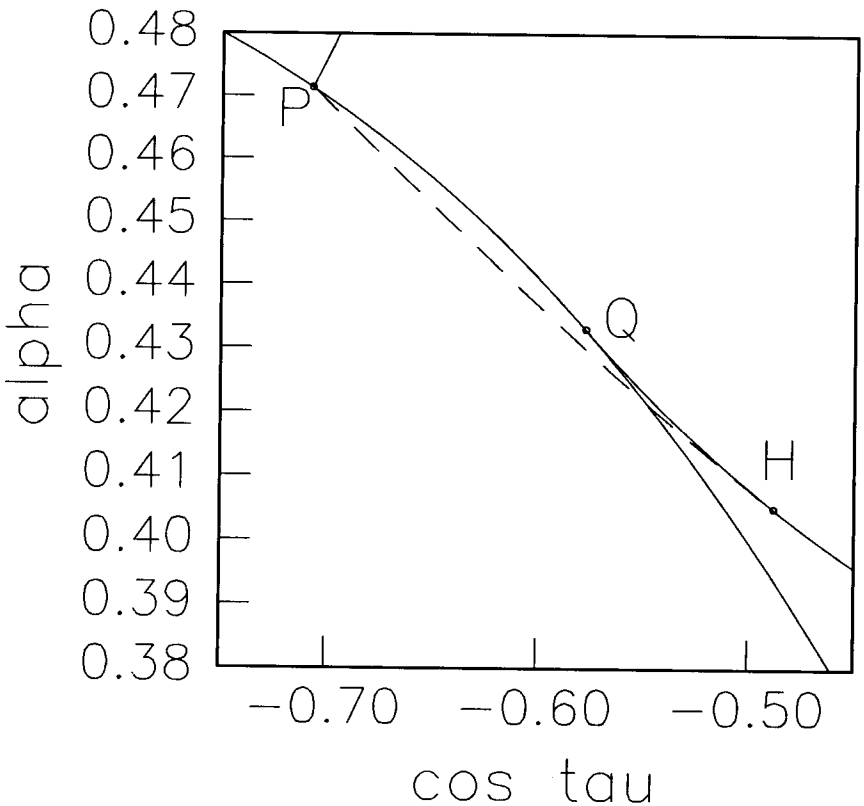

Figure 3. Enlargement of a region of Figure 2 showing the curve of Hopf bifurcations, eq.(30), as a dashed line. The curve connecting points P and Q is eq.(23). The curve connecting points Q and H is eq.(28).

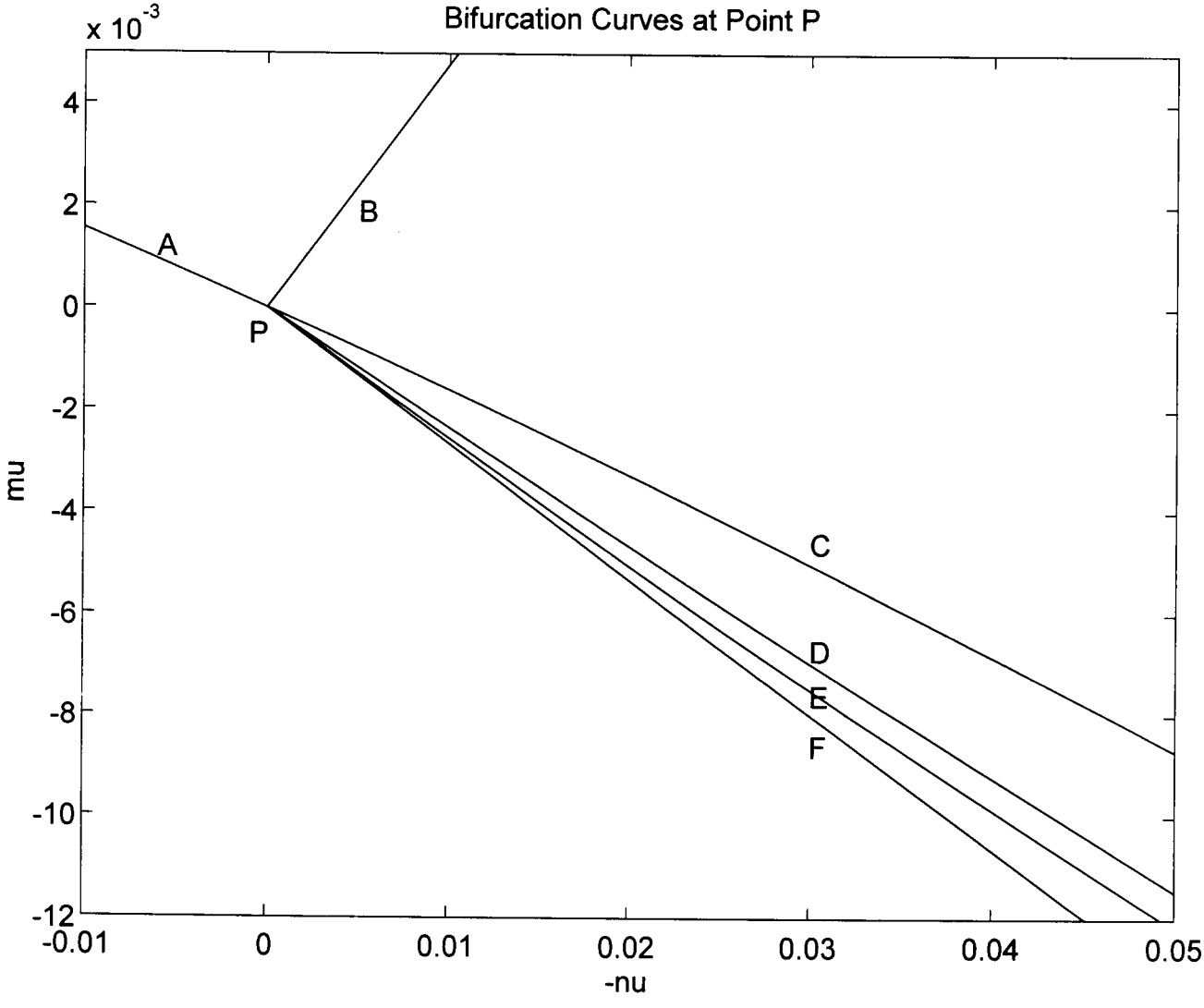

Figure 4. Bifurcation curves at point P obtained via center manifold analysis and normal forms. The eqs. for curves A,B,C,D,E,F are given in (33)-(37). Each of these curves separates regions of parameter space containing qualitatively distinct phase portraits, see Figure 5.

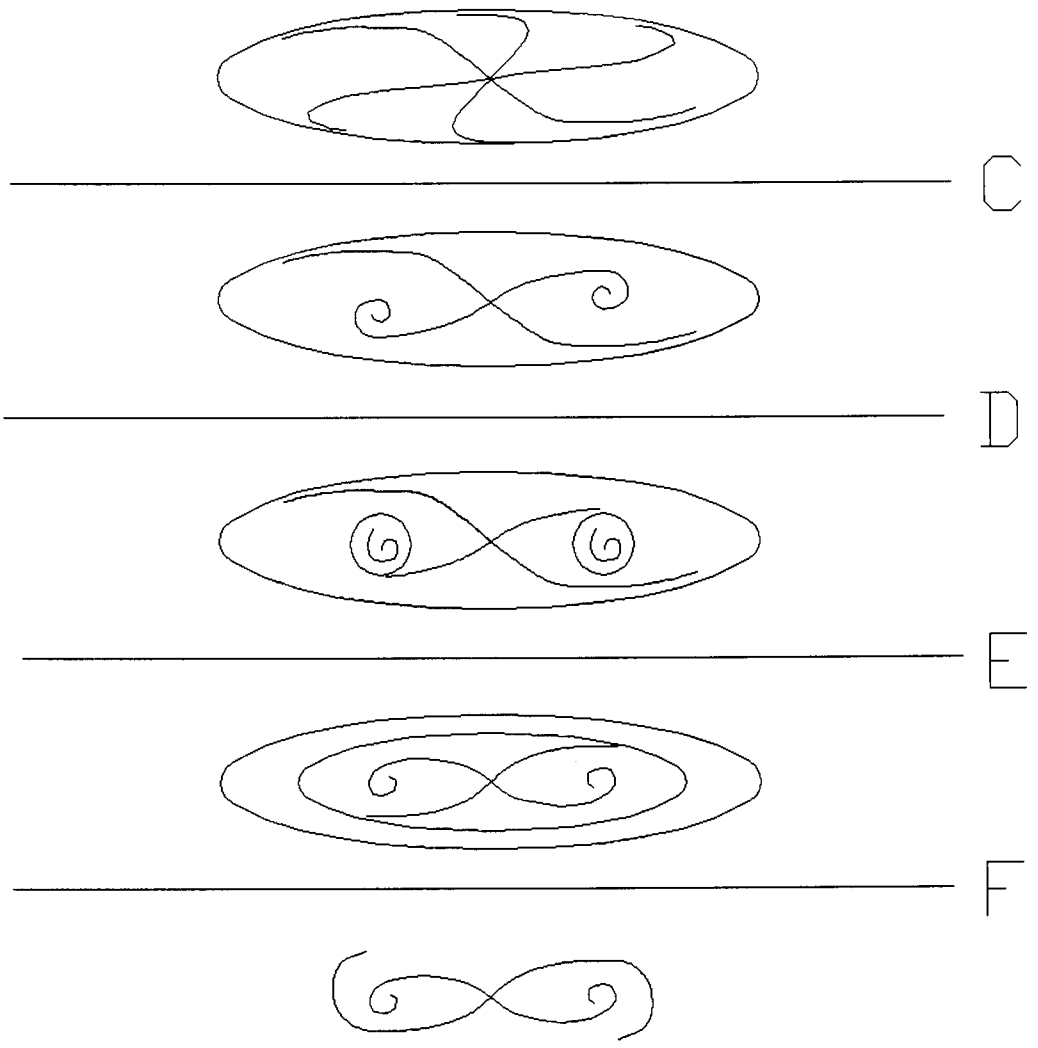

Figure 5. Schematic diagram showing the qualitatively distinct center manifold phase portraits found in the parameter space near point P. The letters C,D,E,F correspond to the bifurcation curves shown in Figure 4. In the region above curve C we have a stable equilibrium (the in-phase mode) and an unstable limit cycle. As we cross the pitchfork bifurcation represented by curve C, the in-phase mode becomes unstable and two stable equilibria are born. Continuing down the page, these two newly created equilibria become unstable and two stable limit cycles are born as we cross the supercritical Hopf bifurcation D. Curve E is a symmetry-breaking bifurcation in which a homoclinic connection replaces the two smaller limit cycles with a single large stable limit cycle. Finally the stable and unstable limit cycles coalesce as we cross the limit cycle fold F, leaving us with three unstable equlibria. Note that in addition to all these steady states, the phase space also contains a stable equilibrium corresponding to the out-of-phase mode.